CHAPTER II
LITERATURE REVIEW

2.1 Plasma Technology

2.1.1 Basic Principle

Plasma state is a mixture of gases consisted of charged particles with a roughly zero net electrical charge. When apply a high energy source, like electric field, to a high voltage (HV) electrode, an ionization process occurs, thus generating a number of ionized species. The plasma has been used to modify the surfaces of both inorganic and organic substrates. This technique is a dry process and is operated under a wide range of pressure. Moreover, the surface modification by the plasma treatment occurs at the outermost surface, so it does not change the bulk properties of materials. Due to its several advantages over the conventional chemistry methods, the plasma becomes more interested.

2.1.2 Classification of Plasma

The plasma is classified into two main states: hot plasmas (thermal plasmas, or equilibrium plasmas) and cold plasmas (non-thermal plasmas, or non equilibrium plasmas).

2.1.2.1 Hot Plasmas

The hot plasmas are consisted of electrons and heavy particles generated at a high temperature so they are high temperature gases (usually higher than 10,000 K). The sufficiently high working pressures and low electric fields are used to generate hot plasmas. In hot plasmas, the temperature of electron (T_e) is approximately equal to neutral temperature (T_n), ($T_e \approx T_n$) and the maximal degree of ionization is close to 100 %. These plasmas are sustained at high power densities (power input per unit volume) and have low chemical selectivity. The overheating of reaction occurs when energy is consumed by the reagents into all degree of freedom so high energy consumption required to provide special quenching of the reagents is the main drawbacks of hot plasmas in the point of view of their chemical applications. The hot plasmas include electrical arc, plasma jets of rocket engines, thermo-nuclear reaction generated plasma, etc.

2.1.2.2 Cold Plasmas

In cold plasmas, the temperature of heavy particles — charged, neutral molecular, and atomic species — are low but the temperature of electrons are high. Normally, the temperature is in the range of 10,000 K to 50,000 K. This plasma type has negligible heat capacity because the free electrons contain much less than one million of the total mass of the system. However, the actual heat content of the plasma is low (Fridman and kennedy, 2004; Shishoo, 2007). The degree of ionization is about 10^{-4} % to 10 %. According to these characteristics, cold plasmas are appropriate for modifying organic surfaces. The cold plasmas are generated by low pressure direct current (DC) and radio frequency (RF) discharges (silent discharges), as well as discharge from fluorescent (neon) illuminating tubes. Other types of cold plasmas are auroras, microwave (MW) discharge, corona discharge, and dielectric DBD plasma. The latter is used in the present study because it provides many advantages, including the reduction of processing cost and the high production rate.

2.1.3 DBD Plasma

The DBD plasma was invented by Siemens in 1857. The discharged plasmas are generated by a number of individual filaments. The breakdown channel (micro-discharges) is controlled and the DBD process is optimized for appropriate applications. The DBD plasma system is composed of DBD reactor, energy source, metallic electrode (such as aluminum, copper, etc.), and dielectric material (such as glass, quartz, ceramic, etc).

Generally, dielectric material is covered either at one side of electrode or both of them. The dielectric materials have two functions: (1) to limit the discharge current and avoid the arc transition, and (2) to ensure a homogeneous treatment by distributing randomly streamers (Tendero *et al.*, 2006).

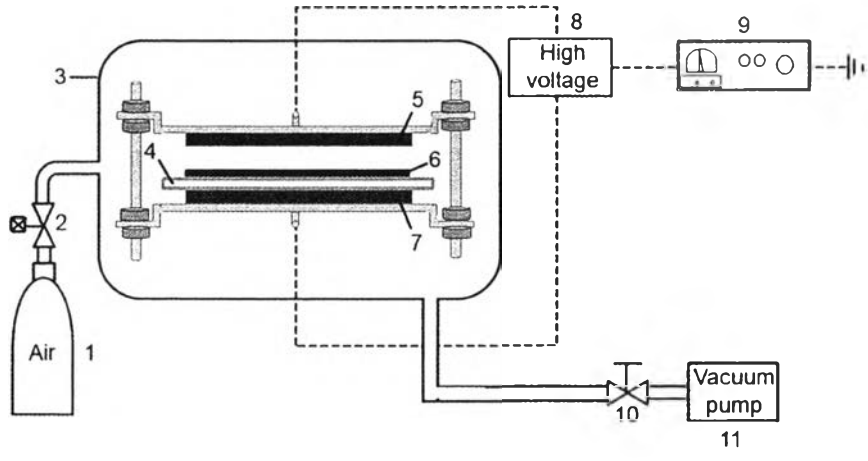

Figure 2.1 Schematic view of the DBD system used for the surface modification (1. air gas cylinder, 2. mass-flow controller, 3. plasma chamber, 4. glass dielectric layer, 5. upper electrode, 6. polyethylene film, 7. lower electrode, 8. high voltage, 9. power supply, 10. needle calve, and 11. vacuum pump) (Geyter *et al.*, 2007).

To initiate and sustain the generated electrons in the DBD system, the energy sources are important. The energy source in DBD system can be alternative current (AC), DC, RF, and MW. After applying the energy to HV electrode, the electrons from metallic electrode strike the dielectric material before emitting the electrons in the system. These electrons are subsequently struck at the bond of gas molecules, so the high energetic species are generated. These species are used to modify the substrate surfaces. The lower electrode is ground electrode which is connected to the resistor.

The DBD plasma technique has been used for the surface modification of various types of polymeric substrates for different purposes, such as to enhance the compatibility of dissimilar polymer surface, to improve deposition of thin film, to etch the polymer surfaces, and to modify the hydrophilic, wetability, and printability properties of the polymeric surfaces. The polymeric materials in food packagings — such as poly(ethylene terepthalate) (PET) (Esena *et al.*, 2005), polypropylene (PP) (Bongiovanni, 2007; Leroux, 2008; Chiang, 2010), polyethylene (PE) (Ren *et al.*, 2008), and polylactic acid (PLA) (Geyter *et al.*, 2010) — have been surface-modified with the DBD plasma.

Esena *et al.* (2005) modified the PET film by using the DBD plasma generated at atmospheric pressure. The plasma source is RF, while typical power during the treatment ranged from 150 W to 300 W. The results of water contact angle measurement and the atomic force microscopy (AFM) indicated that the wettability, printability, and roughness of the PET surface increased after the plasma treatment. These changes improved the adhesion of surface coating and deposition.

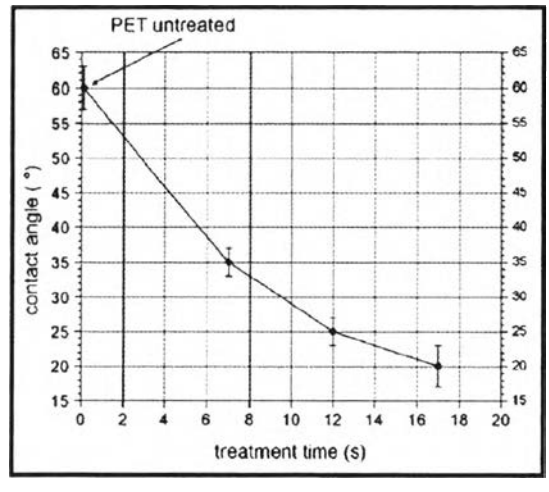

Figure 2.2 Water contact angles of PET film as a function of DBD plasma treatment time (Esena *et al.*, 2005).

Liu *et al.* (2005) modified the surface of poly(methylmethacrylate) (PMMA) film with the use of DBD plasma. The operating parameters of DBD plasma, including discharge power, electrode gap, and duration of exposure, were investigated. The results showed that a short exposure treatment time significantly changed water contact angle and surface oxygen content of the PMMA film. Moreover, the number of plasma treatment cycles and the treating speed increased the surface wettability of the PMMA film. On the other hand, the plasma power did not affect the surface wettability but increased the amount of oxygen incorporated into the treated surface. Thus, it was also reported that the operating conditions significantly affected changes in chemical and microstructure of those polymeric surfaces.

Bongiovanni *et al.* (2007) modified the surface of PP film by using Ar plasma to improve the adhesion of a highly fluorinated ultraviolet (UV)-cured coating for grafting 2-hydroxyl-2-methyl-1-4-(2-acryloyloxethoxy)-phenyl-propanone (APP) molecules on PP. The operating conditions were at a plasma treatment time of 30 s, a current of 25 W, and gas pressure of 1.5 Torr. The APP molecules gave the cleavage at the α-position to the carbonyl groups so the radical polymerization took place and continuous fluorination occurred.

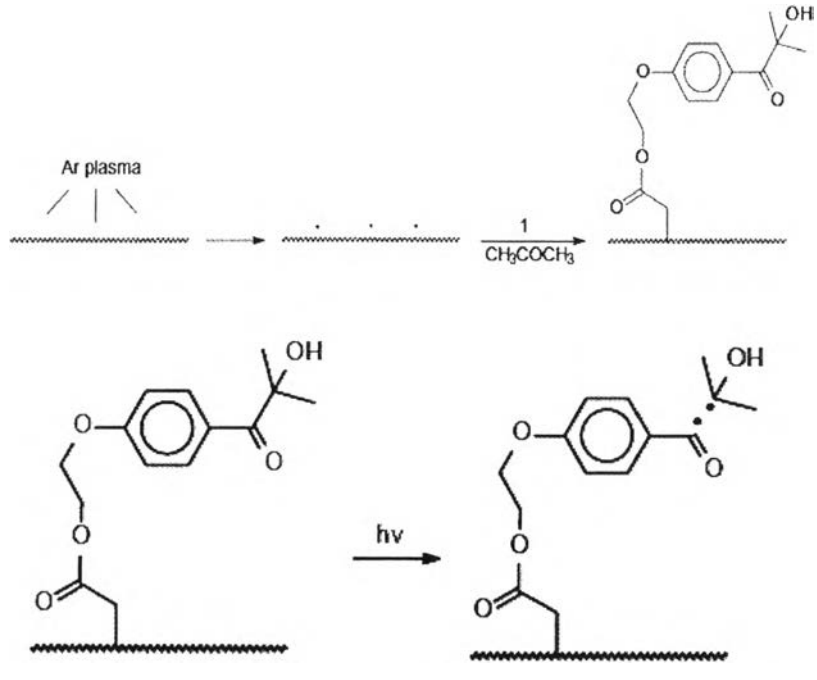

Figure 2.3 Schematic representation of two reaction steps (Bongiovanni *et al.*, 2007).

Leroux *et al.* (2008) treated the PP film by using the DBD plasma generated at atmospheric pressure in order to modify the chemical and physical characteristics of PP surface. From the X-ray photoelectron spectroscopy (XPS) result, the carboxyl groups on the PP film disappeared, so carbonyl and hydroxyl group percentages decreased. It was also found that the air plasma oxidized the

surface of PP film, and increased the surface roughness of the film which was clearly seen from the AFM micrographs, as shown in Figure 2.4.

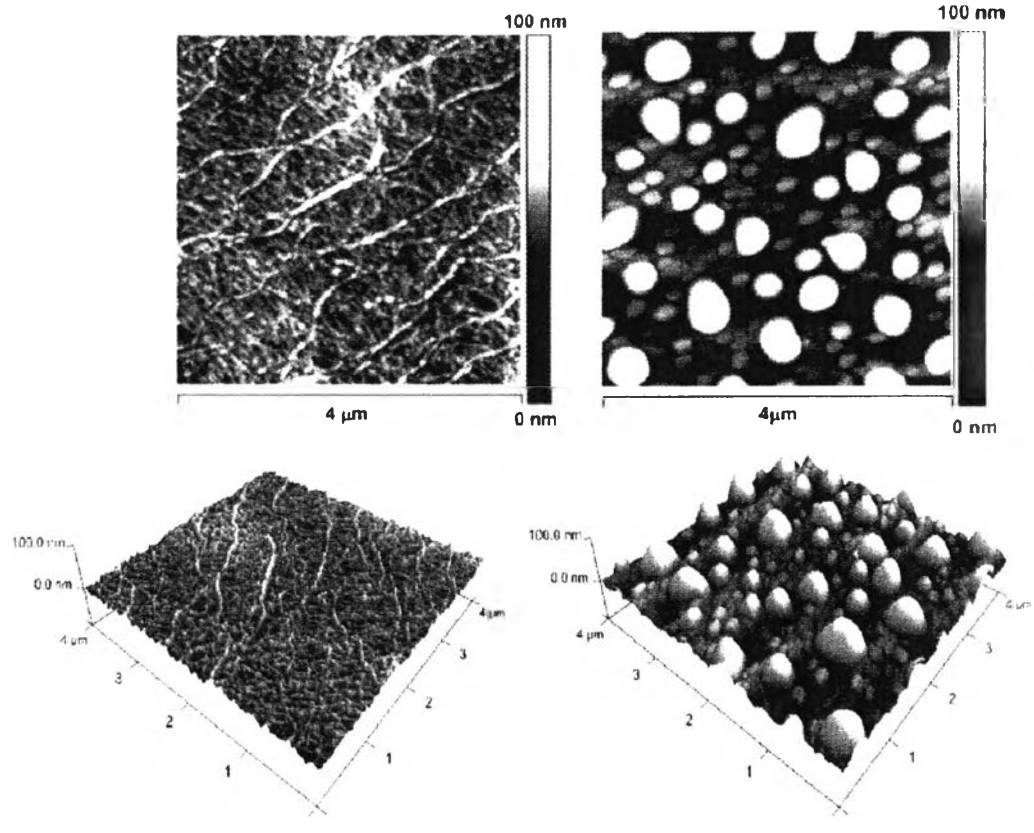

(a) (b)

Figure 2.4 AFM top view and 3D imaging of the PP film: (a) before plasma treatment and (b) after 42 kJ m^{-2} plasma treatment (Leroux *et al.*, 2008).

Ren *et al.* (2008) modified the surface of PE film by using DBD plasma generated in air. Compared to the neat PE film, the chemical composition of the film changed after the plasma treatment. The oxygen functional groups — such as C–O, C=O, O–C=O, and CO_3 — were observed at the film surface. Moreover, the equilibrium between oxidation reaction and etching reaction occurred when the treatment time was longer than 30 s.

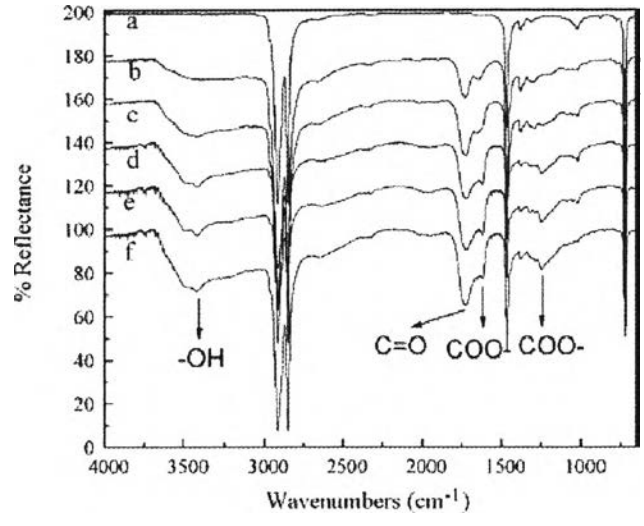

Figure 2.5 Attenuated total reflection-Fourier transform infrared (ATR-FTIR) spectra of (a) untreated PE film and PE film after DBD plasma treatment at (b) 1 s, (c) 10 s, (d) 20 s, (e) 30 s , and (f) 40 s (Ren *et al.*, 2008).

Chiang *et al.* (2010) modified the surface of PP film by using a parallel plate nitrogen-based DBD jet operated at atmospheric pressure. The PP sample was treated with mixture of oxygen (O_2) and nitrogen (N_2) gases at various O_2/N_2 ratios ranging from 0 % to 1.6 % at different gap distances. The hydrophilic properties of both pristine and treated PP films were characterized by contact angle measurement. The result showed that the surface of PP film was effectively modified at a wide range of O_2/N_2 ratios (<1%) and at a gap distance less than 10 mm.

Geyter *et al.* (2010) investigated the surface modification of PLA film From the XPS result, a number of oxygen-containing groups were observed in the cases of air and Ar plasma-treated PLA films. Meanwhile, the N_2 plasma treatment leaded to the incorporation of the nitrogen-containing groups into the PLA surface. Surprisingly, the He plasma added a few of nitrogen-containing groups.

Table 2.1 Atomic composition and concentration of different chemical bonds on untreated and plasma-treated PLA films (energy density of 4.3 J cm^{-2}) (Geyter *et al.*, 2010)

Treatment	%C	%O	%N	O/C	N/C	285.0 eV	286.8 eV	289.1 eV
No	68.2	31.8	0	0.47	0	49.6	25.4	25.0
Air plasma	62.2	37.8	0	0.61	0	38.1	30.5	31.4
Nitrogen plasma	62.1	31.1	6.8	0.50	0.11	41.8	29.1	30.1
Argon plasma	65.1	34.9	0	0.54	0	45.6	28.3	26.1
Helium plasma	66.9	30.4	2.7	0.45	0.04	47.4	26.5	26.1

2.2 ZnO Particles

2.2.1 Basic Properties and Applications

ZnO has been widely studied since 1935 and its unique properties have been intensively reviewed. ZnO is a metal oxide, and the Zn-O is bonded with a very strong ionic character (Jagadish *et al.*, 2006). Furthermore, it has gained more attention in many applications, such as food packaging, catalysis, sensors, environmental remediation, medicine, and personal care (Tayel *et al.*, 2010; Raghupathi *et al.*, 2011), because it is believed to be nontoxic, biological safety, and biocompatible. In packaging applications, ZnO provides several advantages, such as oxygen barrier property and antibacterial activity. It also acts as an UV absorber as well as a filler to enhance the mechanical property (Bachari *et al.*, 2001; Zhao and Li, 2006).

ZnO has wide band gap energy equal to 3.36 eV, which absorbs the UV-light at below 380 nm (Padmavathy *et al.*, 2008). There are two crystallinity forms of ZnO: wurtzite and zincblend. (Figure 2.6) The wurtzite structure is a kind of hexagonal unit cell which the lattice parameters of a equal to 3.2495 Å and c equal to 5.2069 Å while the zincblend structure is a cubic unit cell which the lattice parameters of a equal to b equal to c (Jagadish *et al.*, 2006).

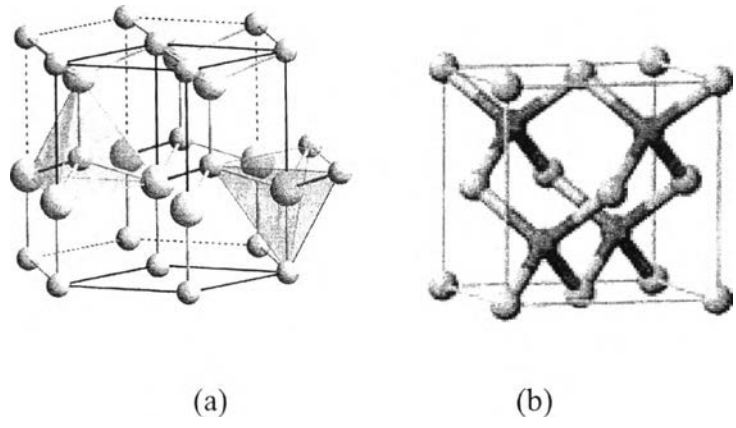

Figure 2.6 Wurtzite (a) and zincblend phases (b) of ZnO (Jagadish *et al.*, 2006).

2.2.2 ZnO Syntheses

There are many methods to synthesis ZnO, such as alkaline precipitation, organic-zinc hydrolysis, and spray pyrolysis. The different synthesis methods and conditions yield ZnO with different morphologies.

2.2.2.1 Alkaline Precipitation

This procedure is used to synthesize ZnO at room temperature by mixing zinc nitrate ($Zn(NO_3)_2$) or zinc acetate ($Zn(CH_3COO)_2$) with alkaline solutions, such as ammonium hydroxide (NH_4OH), sodium hydroxide (NaOH), and potassium hydroxide (KOH). After a drop-wise addition of alkaline solutions, the white particles of ZnO are obtained.

2.2.2.2 Organo-Zinc Hydrolysis

The organo-zinc, such as zinc *t*-butoxide, is used as a precursor by mixing *t*-butanol with diethylzinc hexane solution, thus yielding the ZnO particles.

2.2.2.3 Spray Pyrolysis

This procedure is used to synthesize the ZnO particles at high temperatures (Li and Haneda, 2003).

2.2.3 Antimicrobial Activities of ZnO

The antimicrobial activities of ZnO have been interested since it inhibits the microbial growth or kills microorganisms either with or without UV light. There are many proposed mechanisms for the antimicrobial activities of ZnO.

Nevertheless, the two widely accepted mechanisms are: (1) the ZnO produces the reactive oxygen species (ROS), which are predominantly hydroxyl radicals and superoxide, and (2) the ZnO particles accumulate at the cell membrane. Both mechanisms lead to disorganization of the microbial cell membrane, thus inhibiting the microbial growth or killing the bacterial cells.

$$ZnO + hv \longrightarrow ZnO\ (e^-_{CB} + h^+_{VB}) \quad (1)$$

$$h^+_{VB} + H_2O\ (OH^-) \longrightarrow \bullet OH \quad (2)$$

$$e^-_{CB} + O_2 \longrightarrow \bullet O^-_2 \quad (3)$$

Figure 2.7 Proposed mechanism for the ROS formation (Moafi *et al.*, 2011).

Generally, the antimicrobial activities of ZnO particles are frequently tested against Gram-negative *E. coli* and Gram-positive *S. aureus* bacteria. Surprisingly, *S. aureus* are found to be more resistant than *E. coli* because a higher content of ZnO is required to inhibit the bacterial growth or to kill this Gram-positive bacterium. A lower antimicrobial activity of ZnO against *S. aureus* is mostly likely due to the fact that *S. aureus* produces the oxidative stress responsive gene products, such as superoxide, which dismutase against the ROS produced by ZnO particles (Raghupathi *et al.*, 2011).

Regardless of the antimicrobial activities, ZnO also acts as a photoprotective, thus extending the shelf-life of polymeric materials. Bachari *et al.* (2001) investigated the photoprotective property of ZnO coated on PET film. The formation of stable photo-oxidation products was confirmed by the absorbance peaks in the FTIR spectra located at wavenumbers of 1780 cm^{-1} and 3260 cm^{-1}. As an example, according to Figure 2.8, the photodegradation of PET films is decreased after the ZnO coating.

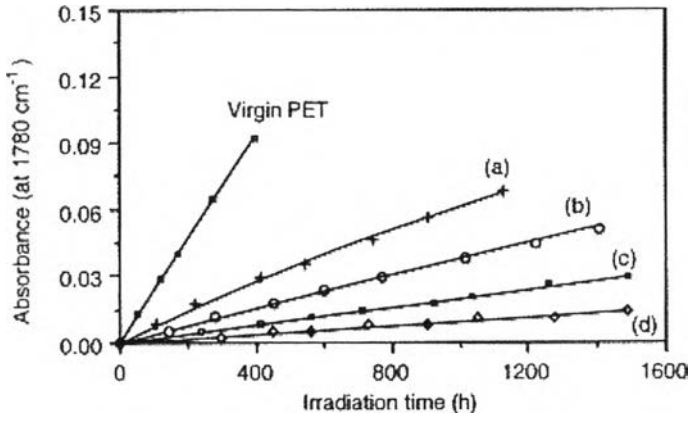

Figure 2.8 Absorbance at a wavenumber of 1780 cm^{-1} in the FTIR spectra of PET films with ZnO deposition elaborated under various irradiation time; the oxygen partial pressure, the total pressure, and the radio frequency power are, respectively: (a) 0.01 and 1 Pa, 0.38 W cm^{-2} ; (b) 0.01 and 1 Pa, 0.64 W cm^{-2} ; (c) 0.05 and 1 Pa, 1.27 W cm^{-2} ; (d) 0.01 and 1 Pa, 1.27 W cm^{-2} (Bachari *et al.*, 2001).

Ghule *et al.* (2006) prepared ZnO nanoparticles-coated paper and studied its antibacterial activity against *E. coli* strain 11634. According to Table 2.2, the highest antibacterial activities are obtained after exposure to UV light at a wavelength of 543 nm (a representative of household fluorescent light) for 24 h. The results also showed that the antibacterial activities increased with increasing exposure time. It should be noted that the viable bacteria were monitored by counting the number of colony-forming units (CFU).

Table 2.2 Antibacterial activity of ZnO nanoparticles-coated paper against *E. coli* strain 11634 (Ghule *et al.*, 2006)

	Bacteria count (CFU) after seeding and washing immediately	Bacteria count (CFU) on illumination with 365 nm light (1 mW cm^{-2}, 1 h)		Bacteria count (CFU) on illumination with 365 nm light (1 mW cm^{-2}, 3 h)		Bacteria count (CFU) on illumination with 543 nm, 1000 lux ≈ 0.1464 mW cm^{-2}, 24 h	
		In light	No light	In light	No light	In light	No light
Blank (white cotton)	1.1×10^5	2.6×10^5	6.4×10^5	2.4×10^6	5.0×10^6	2.4×10^8	2.7×10^8
Blank paper	1.1×10^4	1.3×10^3	2.0×10^4	4.8×10^3	1.5×10^5	3.7×10^6	5.4×10^6
ZnO nanoparticles coated paper	1.0×10^4	1.6×10^2	3.2×10^2	1.3×10^2	1.2×10^4	<20	<20

The particle size of ZnO also affects the inhibition of bacterial growth. Tayel *et al.* (2011) studied the antibacterial activities of ZnO nanoparticles compared with those of conventional ZnO powders. Both of them were tested against Gram-positive and Gram-negative bacteria. From Table 2.3, it might be concluded that the antibacterial activities of ZnO nanoparticles are stronger than those of ZnO powders because ZnO nanoparticles has larger surface areas.

Table 2.3 Antibacterial activities of ZnO powders and nanoparticles against various types of bacterial strains as indicated by diameter of inhibition zone and minimal inhibitory concentration (MIC)

	ZnO powder		ZnO nanoparticle	
Bacterial strain	Zone diameter*	MIC (mM)	Zone diameter	MIC (mM)
Bacillus cereus	18 ± 1.1	17	35 ± 1.6	7
Enterobacter cloacae	14 ± 0.9	74	19 ± 1.4	21
Escherichia coli	12 ± 0.8	68	21 ± 1.3	16
E. coli O157:H7	13 ± 0.6	64	18 ± 1.1	17
Pseudomonas aeruginosa	11 ± 0.4	72	17 ± 1.2	26
Pseudomonas fluorescens	9 ± 0.3	80	18 ± 1.1	24
Salmonella enteritidis	11 ± 0.5	54	22 ± 1.2	20
Salmonella typhimurium	12 ± 0.6	66	21 ± 1.4	22
Staphylococcus aureus	17 ± 1.2	19	31 ± 1.4	10